Dual Excitation Behavior of Double Proton Transfer versus Charge Transfer in 4-(N-Substituted Amino)-1H-pyrrolo[2,3-*b*]pyridines Tuned by Dielectric and Hydrogen-bonding Perturbation

Pi-Tai Chou,*,† Yun-I Liu, Hsiao-Wei Liu, and Wei-Shan Yu

Department of Chemistry
The National Chung-Cheng University
Chia Yi, Taiwan R.O.C.

Received August 3, 2001

The excited-state double proton transfer (ESDPT) process in 7-azaindole (7AI) dimer has long been recognized as one possible mutation mechanism due to a misprint induced by the proton-transfer tautomerism of a specific DNA base pair.[1b] Much research has focused on dynamics of ESDPT incorporating various types of guest molecules (including 7AI).[1−11] Focus on the chemical modification of 7AI has also been of particular interest to study ESDPT toward biochemical application.[9,10d] Herein, on the basis of the synthesis of 4-(dimethylamino)-1H-pyrrolo[2,3-*b*]pyridine (DPP[12]) and its analogues, we demonstrate the remarkable dual excitation behavior of proton-transfer versus charge-transfer fined-tuned by dielectric as well as hydrogen-bonding perturbation.[14]

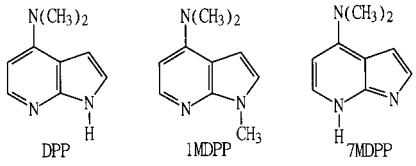

When the concentrations were increased, the absorption spectra of DPP revealed red-shift with the appearance of a new peak maximum at 310 nm (see Figure 1A). In comparison, the absorption features of 1-methyl-4-(dimethylamino)-1H-pyrrolo[2,3-b]pyridine (1MDPP[15]) showed concentration independence. The results demonstrate the formation of a DPP dimer through a dual hydrogen-bonding effect. On the basis of the similar equation derived from self-association of 7AI,[1b] a large dimerization constant of 4.2×10^3 M^{-1} in cyclohexane was obtained. The monomer exhibited a very weak emission maximum at 327 nm (the F_B band, $\tau_f \approx 70$ ps), while a large Stokes-shifted emission maximum at 440 nm (the F_A band, $\tau_f \approx 2.8$ ns) gradually appeared upon increasing concentration (Figure 1B). The excitation spectrum of the F_A band was red-shifted by ∼10 nm relative to that of the F_B band. These in combination with system-response-limit rise time[14] for both bands demonstrate that they originate from different ground-state species and that one cannot be the precursor of the other. In comparison 1MDPP exhibited a concentration-independent, normal emission maximum at 328 nm ($\tau_f \approx 85$ ps). In addition, 7-methyl-4-(dimethylamino)-1H-pyrrolo[2,3-b]pyridine (7MDPP[16]), the analogue of proton-transfer tautomer for DPP, revealed a single fluorescence band maximum at 465 nm ($\tau_f \approx 4.1$ ns). Accordingly, the F_B band is ascribed to the monomer emission, while the F_A band can be ambiguously assigned to the tautomer emission resulting from fast ($\gg 30$ ps^{-1}) ESDPT of the DPP dimer.

Remarkable concentration-independent, dual emission was observed for DPP in polar, aprotic solvents (see Figure 1B). The short and long emission bands, specified as F_B and F_A, originating

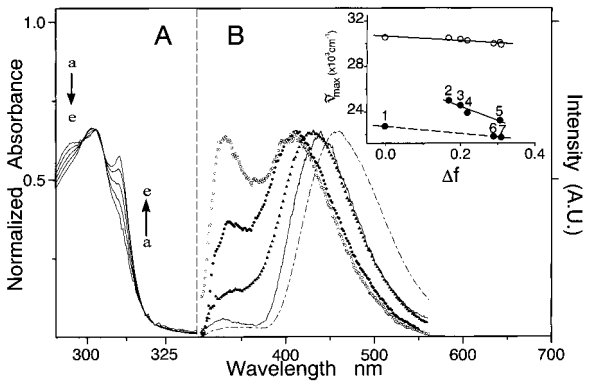

Figure 1. (A) Normalized absorption spectra of DPP at (a) 1.1×10^{-4}, (b) 2.1×10^{-4}, (c) 4.3×10^{-4}, (d) 8.6×10^{-4}, (e) 1.7×10^{-3} M in cyclohexane. (B) Normalized fluorescence spectra of DPP in various solvents: cyclohexane (—, 4.3×10^{-4} M), ethyl acetate (oooo), dichloromethane (●●●●●), acetonitrile (▲▲▲▲), ethanol (— • — •). λ_{ex} = 290 nm. Insert: $\tilde{\nu}_{max}$ of DPP (○: the F_B band, ●: the F_A band) as a function of Δf in 1. cyclohexane, 2. ethyl ether, 3. ethyl acetate, 4. dichloromethane, 5. acetonitrile, 6. ethanol, 7. methanol.

* To whom correspondence should be addressed.
† Current address: Department of Chemistry, National Taiwan University, 106, Taipei, Taiwan.

(1) (a) Taylor, C. A.; El-Bayoumi, A. M.; Kasha, M. *Proc. Natl. Acad. Sci. U.S.A.* **1969**, *65*, 253. (b) Ingham. K. C.; El-Bayoumi, M. A. *J. Am. Chem. Soc.* **1974**, *96*, 1674.
(2) Tokumura, K.; Watanabe, Y.; Udagawa, M.; Itoh, M. *J. Am. Chem. Soc.* **1987**, *109*, 1346.
(3) (a) Douhal, A.; Kim, S. K.; Zewail, A. H. *Nature* **1995**, *378*, 260. (b) Fiebig, T.; Chachisvilis, M.; Manger, M.; Zewail, A. H.; Douhal, A.; Garcia-Ochoa, I.; de La Hoz Ayuso, A. *J. Phys. Chem. A* **1999**, *103*, 7419.
(4) Takeuchi, S.; Tahara, T. *J. Phys. Chem. A* **1998**, *102*, 7740.
(5) McMorrow, D.; Aartsma, T. *Chem. Phys. Lett.* **1986**, *125*, 581.
(6) Moog, R. S.; Bovino, S. C.; Simon, J. D. *J. Phys. Chem.* **1988**, *92*, 6545.
(7) Koijnenberg, J.; Huizer, A. H.; Varma, C. A. O. *J. Chem. Soc., Faraday Trans.* 2 **1988**, *84* (8), 1163.
(8) (a) Moog., R. S.; Maroncelli, M. *J. Phys. Chem.* **1991**, *95*, 10359. (b) Chapman, C. F.; Maroncelli, M. *J. Phys. Chem.* **1992**, *96*, 8430.
(9) (a) Negreie, M.; Bellefeuille, S. M.; Whitham, S.; Petrich, J. W.; Thornburg, R. W. *J. Am. Chem. Soc.* **1990**, *112*, 7419. (b) Negrerie, M.; Gai, F.; Bellefeuille, S. M.; Petrich, J. W. *J. Phys. Chem.* **1991**, *95*, 8663. (c) Chen, Y.; Rich, R. L.; Gai, F.; Petrich, J. W. *J. Phys. Chem.* **1993**, *97*, 1770. (d) Gai, F.; Rich, R. L.; Petrich, J. W. *J. Am. Chem. Soc.* **1994**, *116*, 735. (e) Smirnov, A. V.; English, D. S.; Rich, R. L.; Lane, J. Teyton, L.; Schwabacher, A. W.; Luo, S.; Thornburg, R. W.; Petrich, J. W. *J. Phys. Chem.* **1997**, *101*, 1B, 2758.
(10) (a) Chou, P. T.; Martinez, M. L.; Cooper, W. C.; McMorrow, D.; Collin, S. T.; Kasha; M. *J. Phys. Chem.* **1992**, *96*, 5203. (b) Chou, P. T.; Wei, C. Y.; Chang, C. P.; Chiu, C. H. *J. Am. Chem. Soc.* **1995**, *117*, 7259. (c) Chou, P. T.; Wei, C. Y.; Chang, C. P.; Kuo, M. S. *J. Phys. Chem.* **1995**, *99*, 11994. 13. (d) Chou, P. T.; Wei, C. Y.; Wu, G. R.; Chen, W. S. *J. Am. Chem. Soc.* **1999**, *121*, 12186.
(11) For theoretical approaches, see: (a) Mente, S.; Maroncelli, M. *J. Phys. Chem. A* **1998**, *102*, 3860. (b) Guallar, V.; Batista, V. S.; Miller, W. H. *J. Chem. Phys.* **1999**, *110*, 9922. (c) Catalán, J.; Del Valle, J. C.; Kasha, M. *Proc. Natl. Acad. Sci. U.S.A.* **1999**, *96*, 8338. (d) Chaban, G. M.; Gordan, M. S. *J. Phys. Chem. A* **1999**, *103*, 185. (e) Fernández-Ramos, A.; Smedarchina, Z.; Siebrand, W.; Zgierski, M. Z.; Rios, M. A. *J. Am. Chem. Soc.* **1999**, *121*, 6280. (f) Kyrychenko, A.; Stepanenko, Y.; Waluk, J. *J. Phys. Chem. A* **2000**, *104*, 9542.
(12) . The synthesis of DPP was according to a previous report.[13] The crude product was worked up by flash column chromatography (eluent: 10−20% methanol by weight in dichloromethane) to obtain DPP. ^{1}H NMR (200 MHz, $CDCl_3$) δ 6.18 (d, J = 6 Hz, 1H), 6.64 (d, J = 3.8 Hz, 1H), 7.12 (d, J = 3.8 Hz, 1H), 7.96 (d, J = 6.0 Hz, 1H).
(13) (a) Schneller, S. W.; Luo, J. K. *J. Org. Chem.* **1980**, *45*, 4045. (b) Girgis, N. S.; Larson, S. B.; Robins, R. K.; Cottam, H. B. *J. Heterocycl. Chem.* **1989**, *26*, 317.
(14) Time-resolved measurements were achieved by using the second or third harmonic of the Ti−sapphire oscillator (100 fs, 82 MHz, Spectra Physics) as an excitation source coupled with a pulse picker (NEOS, model N17389). An Edinburgh OB 900-L single photon counter was used as a detecting system, giving a temporal resolution of ∼30 ps.
(15) 1MDPP was synthesized by adding sodium hydride (100 mg) to the THF solution containing DPP (0.15 g), followed by the addition of methyl iodide (100 mg). ^{1}H NMR (200 MHz, $CDCl_3$) 3.28 (s, 6H), 3.89 (s, 3H), 6.20 (d, J = 6 Hz, 1H), 6.62 (d, J = 3.6 Hz, 1H), 6.94 (d, J = 3.6 Hz, 1H), 8.03 (d, J = 6 Hz, 1H).
(16) 7MDPP was synthesized by the reaction of DPP (0.1 g) and methyl iodide (0.5 g) in THF, followed by the addition of NaOH (2.5 N, 10 mL). ^{1}H NMR ($CDCl_3$, 400 MHz) δ 3.38 (s, 6H), 4.08 (s, 3H), 6.05 (d, J = 7.2 Hz, 1H), 6.76 (d, J = 2.8 Hz, 1H), 7.35 (d, J = 7.2 Hz, 1H), 7.47 (d, J = 2.8 Hz, 1H).

10.1021/ja011881s CCC: $20.00
Published on Web 11/08/2001

Table 1. Physical Parameters of Solvents as Well as Photophysical Properties of DPP, 1MDPP[a] in Various Solvents at 298 K

		($\times 10^4$ cm^{-1})		($\times 10^{-3}$)	($\times 10^{-2}$)		
solvent	Δf	$\tilde{\nu}_B$	$\tilde{\nu}_A$	Φ_B[b]	Φ_A[b]	τ_B(ps)[c]	τ_A(ns)[c]
CHE	~0.0	3.054(3.043)	2.272(NA)	0.92(1.36)	10.31	70(85)	2.80
ether	0.168	3.042(3.038)	2.500(2.514)	2.19(1.81)	0.11(0.07)	102(95)	0.31(0.15)
EA	0.199	3.037(3.001)	2.457(2.471)	1.31(2.60)	0.23(0.10)	80(128)	0.35(0.18)
DCM	0.218	2.998(2.984)	2.392(2.405)	2.68(3.11)	0.67(0.15)	120(131)	0.51(0.22)
ACN	0.306	2.985(2.980)	2.325(2.331)	2.37(3.07)	2.08(0.65)	110(162)	2.30(1.18)
EtOH	0.289	2.990(2.981)	2.183(2.262)	2.08(2.50)	6.67(0.68)	50(55)	0.22[d]
							3.60(1.33)
MeOH	0.309	2.982(2.972)	2.175(2.212)	1.01(1.70)	2.74(0.49)	42(48)	0.17[d]
							3.17(1.05)
H_2O[e]	0.320	2.825(2.817)	2.096(2.105)	0.65(1.19)	0.11(0.09)	NA(35)	0.30(0.29)

[a] Data for 1MDPP listed in parentheses. [b] Apparent yields without considering the branching ratio for populating F_B versus F_A state. [c] Minimum uncertainty of ±15 ps. [d] Rise component. [e] Data were obtained at pH ~10[20].

from a common ground-state species were ascertained by the same fluorescence excitation spectra, which were also identical with the absorption spectrum. Peak frequencies for the F_A band showed strong solvent-polarity dependence. Treating the solute by a spherical cavity, a modified Lippert equation was derived to be $\tilde{\nu}_f = \tilde{\nu}_f^{vac} - (2(\vec{\mu}_e - \mu_g)^2)\Delta f/hca_0^3$ (**1**) where Δf denotes solvent polarity parameter.[17] The insert of Figure 1 shows the linear plot of $\tilde{\nu}_{max}$ versus Δf for both F_B and F_A bands, where the slope for the F_A band (-1.24×10^4 cm^{-1}) is much steeper than that for the F_B band, indicating a large dipolar change between ground and excited states. The lack of a proton-donating site in aprotic solvents excludes the assignment of the F_A band to a proton-transfer tautomer emission. This viewpoint is supported by similar dual emission properties in 1MDPP (see Table 1). Alternatively, the results lead us to propose that the F_A band originates from an excited-state charge transfer (ESCT) incorporating dimethylamine and pyridinic nitrogen.[18] As shown in Table 1 both F_B and F_A bands exhibit response-limited rise, resolvable single-exponential decay dynamics. This in combination with identical excitation spectra suggests that they share a common Franck−Condon state. This initially prepared electronically excited state rapidly relaxes to F_B and F_A states. These two states then undergo independent decay dynamics.[19]

Dual emission maxima were also observed in ethanol. While $\tilde{\nu}_{max}$ of the F_B band lies on the linear plot, the correlation for $\tilde{\nu}_{max}$ of F_A band versus Δf deviates significantly from the linear behavior in aprotic solvents (see insert of Figure 1). The result may indicate that ESCT is operative, but the CT species is subjective to the specific hydrogen-bonding interactions. However, it is more plausibly rationalized by ESDPT phenomena based on several experimental evidences. First, $\tilde{\nu}_{max}$ for the F_A band in DPP (21 830 cm^{-1}) is lower in energy than that in1MDPP (22 625 cm^{-1}) by as large as ~800 cm^{-1} in ethanol, while the difference is negligible in polar, aprotic solvents (see Table 1). Second, a response-limited rise, single-exponential decay component ($\tau_f \approx$ 1.3 ns) was resolved from the F_A band for 1MDPP in ethanol. In contrast, for DPP the F_A band can only be well fitted by dual relaxation dynamics expressed as $F(t) = a_1\ e^{-k_1 t} + a_2\ e^{-k_2 t}$. Independently of the monitored wavelengths, k_1 and k_2 were deduced to be 220 ± 15 ps^{-1} and 3.6 ns^{-1}, respectively. Instead

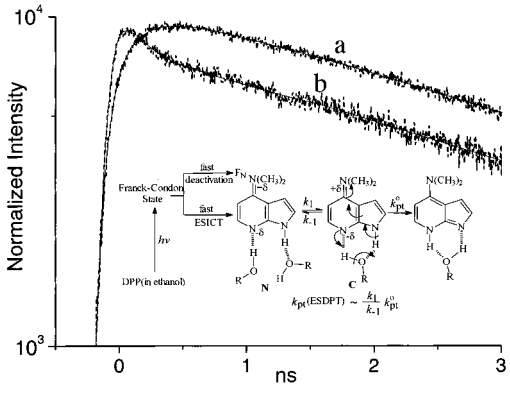

Figure 2. Logarithm plot of the time-dependent fluorescence of DPP in ethanol and its corresponding best-fitted curve. The emission wavelength was monitored at (a) 465 nm, (b) 410 nm. $\lambda_{ex} = 266$ nm. Insert: The proposed ESCT/ESDPT coupled mechanism for DPP in ethanol (R: C_2H_5).

of the positive value for the fitted a_2 throughout the monitored wavelengths the sign of a_1 is wavelength-dependent. When monitoring at >450 nm a negative a_1 was obtained as indicated by a rise component (see Figure 2a), which gradually shifted to a positive value, that is, the appearance of a faster decay component, at shorter wavelength of for example 410 nm (see Figure 2b). $|a_1/a_2|$ was not equal to 1.0 and was found to be wavelength-dependent. For example, this value is deduced to be 0.5 at 465 nm, indicating that ~50% of the fluorescence promptly exists, while the remaining 50% have not yet been populated. The results conclude the existence of two species at >410 nm and one with fast decay of 220 ps is the precursor of the other. Since DPP possesses a parent structure that is similar to that of 7AI that undergoes alcohol-catalyzed proton transfer in the excited state,[1,5−10a] it is reasonable to propose the occurrence of ESDPT for DPP in ethanol, resulting in a proton-transfer tautomer emission. Note a linear plot of $\tilde{\nu}_{max}$ versus Δf was obtained for the F_A band of DPP in cyclohexane, ethanol and methanol (insert of Figure 1), supporting their similar spectral properties.

Since the lifetime of the F_B band was resolved to be as fast as ~50 ps, the precursor of ESDPT mainly originates from the CT state to account for the rise dynamics of 220 ps^{-1} in ethanol. Consequently, a mechanism of ESCT/ESDPT-coupled reaction was proposed. Upon excitation the ESCT takes place, accompanied by fast solvent relaxation dynamics to reach a stabilized CT state within the system-response limit of 30 ps. The equilibrated CT species further undergoes ethanol-assisted, irreversible ESDPT. In steady-state measurements the 442-nm CT band predicted from that of 1DMPP in ethanol is obscured in DPP due to the dominant rate of ESDPT. The rise kinetics (k_{pt}) of the tautomer emission, depending on types of monoalcohols, was measured to be 170 and 250 ps^{-1} in methanol and propanol, respectively. Deuterium isotope effect was observed. k_{pt} was resolved to be ~640 ps^{-1} in ethanol-*d*. The calculated k_{pt}^H/k_{pt}^D ratio of 2.9 is very close to that of ~3.0 reported for 7AI[7,8a,9a,b] in ethanol. Accordingly, the mechanism of alcohol catalyzed ESDPT in DPP should be similar to a two-step mechanism proposed for 7AI,[7−9,11a] incorporating equilibrium solvation between cyclic (structure **C**) and neighbor-bonded structures **N**, followed by a possible proton-tunneling mechanism (see insert of Figure 2). A distinct difference is that the precursor of the ESDPT in DPP is a charge-transfer species, while a neutral species is operative in 7AI. In conclusion we reported the dual excitation behavior, that is, ESDPT versus ESCT in DPP fine-tuned by solvent polarity as well as hydrogen-bonding perturbation, which makes DPP a unique model among hydrogen-bonded complexes to study the interplay between two fundamental mechanisms.

JA011881S

(17) Lippert, E. *Z. Naturforsch.* **1955**, *10a*, 541. In eq **1** $\Delta f = (\epsilon - 1)/(2\epsilon + 1) - (1)/(2)(n^2 - 1)/(2n^2 + 1)$ where ϵ and n respectively denote the static dielectric constant and the refractive index.

(18) Whether the mechanism incorporates twisted intramolecular charge transfer or not requires further investigation. Focus on this issue is in progress.

(19) Detailed relaxation dynamics as well as the branching ratio to populate F_B and F_A states require femtosecond time-resolved measurements.

(20) The pK_a for protonated DPP was determined to be 6.8 at 298 K. Thus, the experiment was performed at pH ≈ 10 where the neutral form dominates in the ground state. Only normal and charge-transfer emission can be resolved. Similar to 7AI in water,[8b,9c−e] the lack of tautomer emission for DPP possibly results from slow proton-transfer dynamics in combination with the dominant radiationless decay.